

Supplemental Materials for

Fe stabilized metallic phase of NiS₂ for highly efficient oxygen evolution reaction

Xingyu Ding,^a Weiwei Li,^b Haipeng Kuang,^a Mei Qu,^a Meiyang Cui,^a Chenhao Zhao,^a Dong-Chen Qi,^d Freddy E. Oropeza^{*c} and Kelvin H. L. Zhang^{*a}

^aState Key Laboratory of Physical Chemistry of Solid Surfaces, College of Chemistry and Chemical Engineering, Xiamen University, Xiamen 361005, P.R. China.

^bDepartment of Materials Science & Metallurgy, University of Cambridge, 27 Charles Babbage Road, Cambridge, CB3 0FS, United Kingdom

^cLaboratory of Inorganic Materials Chemistry, Department of Chemical Engineering and Chemistry, Eindhoven University of Technology, P. O. Box 513, 5600MB Eindhoven, The Netherlands

^dSchool of Chemistry, Physics and Mechanical Engineering, Queensland University of Technology, Brisbane, Queensland 4001, Australia

Email: freddyoropeza@gmail.com and kelvinzhang@xmu.edu.cn

Table S1 The actual doped Fe concentrations in $\text{Fe}_x\text{Ni}_{1-x}\text{S}_2$ measured by inductively coupled plasma mass spectrometry (ICP-MS). The actual x values are calculated using

$$x = \frac{\rho_{\text{Fe}}}{M_{\text{Fe}}} \div \left(\frac{\rho_{\text{Fe}}}{M_{\text{Fe}}} + \frac{\rho_{\text{Ni}}}{M_{\text{Ni}}} \right)$$

the following equation: where ρ represents the concentration of metal element in the solution obtained from ICP-MS, $M_{\text{Fe}} = 55.85 \text{ g mol}^{-1}$, $M_{\text{Ni}} = 58.69 \text{ g mol}^{-1}$.

x in $\text{Fe}_x\text{Ni}_{1-x}\text{S}_2$	The concentrations of metal element from ICP-MS		x in $\text{Fe}_x\text{Ni}_{1-x}\text{S}_2$ from ICP-MS
	ρ_{Fe} (mg L ⁻¹)	ρ_{Ni} (mg L ⁻¹)	
0	0	6.31	0
0.05	0.29	6.23	0.046
0.10	0.48	4.72	0.097
0.15	0.66	3.90	0.151
0.20	1.22	5.34	0.194

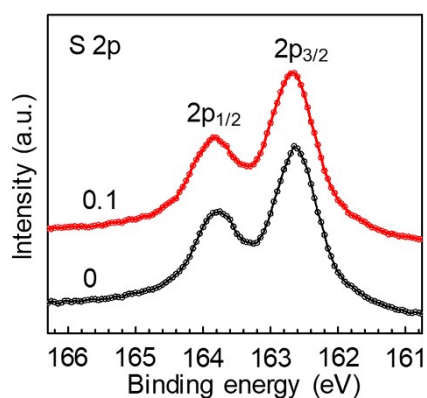


Fig. S1 S 2p XPS spectra of as-synthesized NiS_2 and $\text{Fe}_{0.1}\text{Ni}_{0.9}\text{S}_2$ nanosheets.

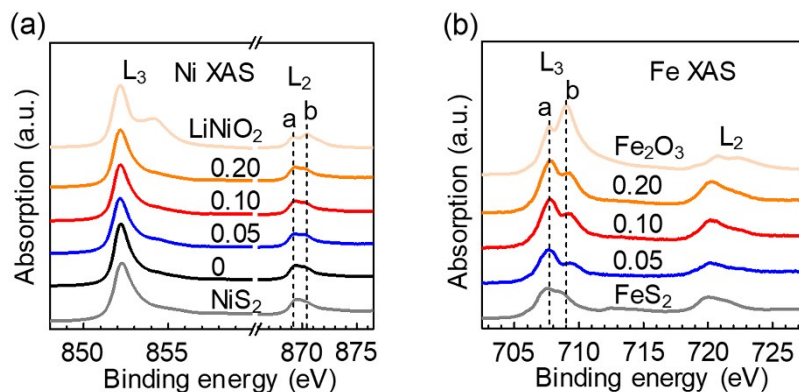


Fig. S2 (a) Ni L-edge XAS spectra of as-synthesized $\text{Fe}_x\text{Ni}_{1-x}\text{S}_2$ ($x=0, 0.05, 0.10$ and 0.20) along with reference spectra of single crystal NiS_2 representing Ni^{2+} and LiNiO_2 representing Ni^{3+} . (b) Fe L-edge XAS spectra of as-synthesized $\text{Fe}_x\text{Ni}_{1-x}\text{S}_2$ ($x=0.05, 0.10$ and 0.20) along with reference spectra of FeS_2 representing Fe^{2+} and Fe_2O_3 representing Fe^{3+} . The results suggest oxidation state of Ni and Fe in $\text{Fe}_x\text{Ni}_{1-x}\text{S}_2$ are consistent with +2.

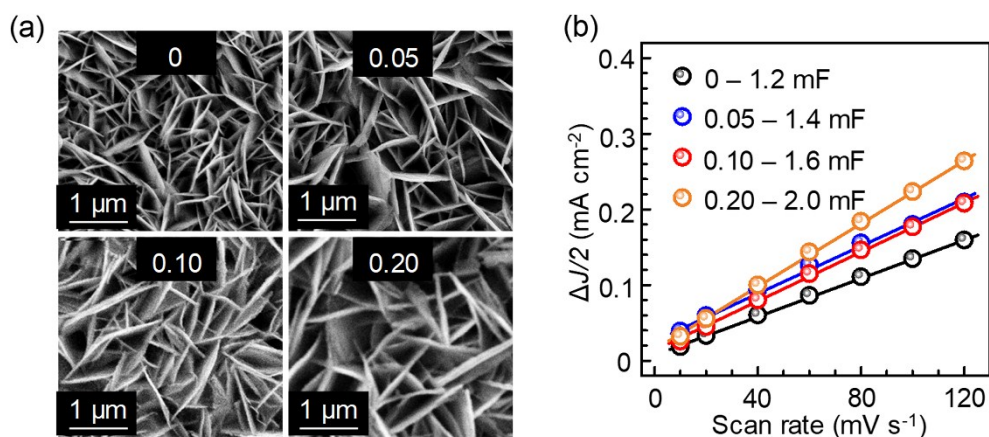


Fig. S3 (a) SEM images of as-synthesized $\text{Fe}_x\text{Ni}_{1-x}\text{S}_2$ ($x=0, 0.05, 0.10$ and 0.20). (b) Plot of current density v.s. scan rates extracted from Fig. S4; the slope is double layer capacitance (C_{dl}) and is proportional to electrochemical active surface area (ECSA). This data suggests all samples have similar ECSA.

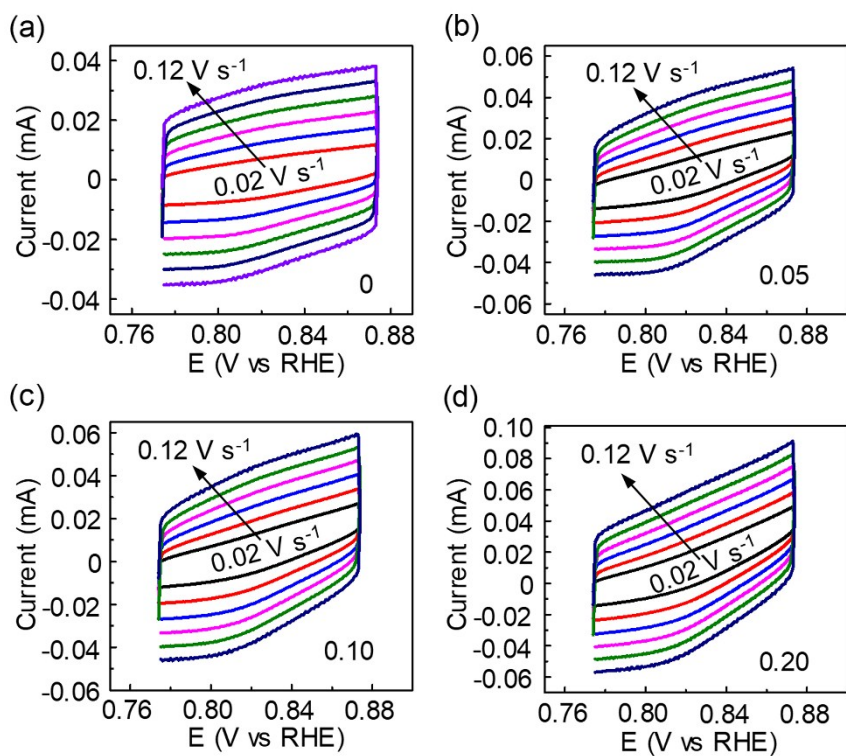


Fig. S4 Cyclic voltammogram of curves of $\text{Fe}_x\text{Ni}_{1-x}\text{S}_2$ with different scan rates (0.02, 0.04, 0.06, 0.08, 0.10, 0.12 V s^{-1}): (a) $x = 0$; (b) $x = 0.05$; (c) $x = 0.10$; (d) $x = 0.20$.

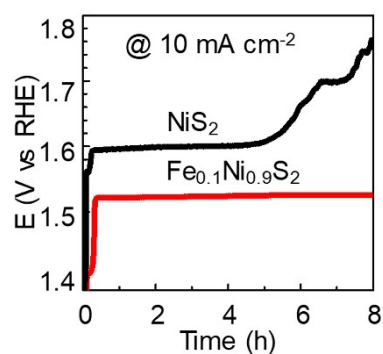


Fig. S5 Chronopotentiometric curves for first 8 hours of NiS_2 and $\text{Fe}_{0.1}\text{Ni}_{0.9}\text{S}_2$ extracted from Fig. 3d.

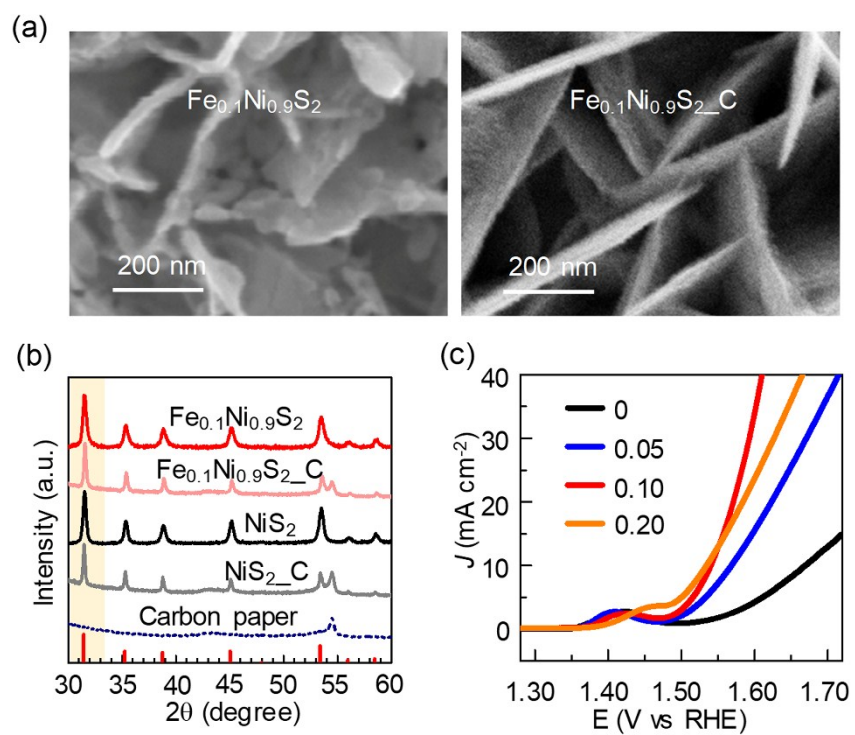


Fig. S6 (a) SEM image of as-synthesized $\text{Fe}_{0.1}\text{Ni}_{0.9}\text{S}_2$ powder (denoted as $\text{Fe}_{0.1}\text{Ni}_{0.9}\text{S}_2$) and $\text{Fe}_{0.1}\text{Ni}_{0.9}\text{S}_2$ prepared on carbon paper (denoted as $\text{Fe}_{0.1}\text{Ni}_{0.9}\text{S}_2\text{-C}$). (b) XRD patterns of the catalysts powder (denoted as NiS_2 and $\text{Fe}_{0.1}\text{Ni}_{0.9}\text{S}_2$) and the catalysts prepared on carbon paper (denoted as $\text{NiS}_2\text{-C}$ and $\text{Fe}_{0.1}\text{Ni}_{0.9}\text{S}_2\text{-C}$). (c) Linear sweep voltammetry (LSV) polarization curves of $\text{Fe}_x\text{Ni}_{1-x}\text{S}_2$ ($x=0, 0.05, 0.10$ and 0.20) prepared on carbon paper.

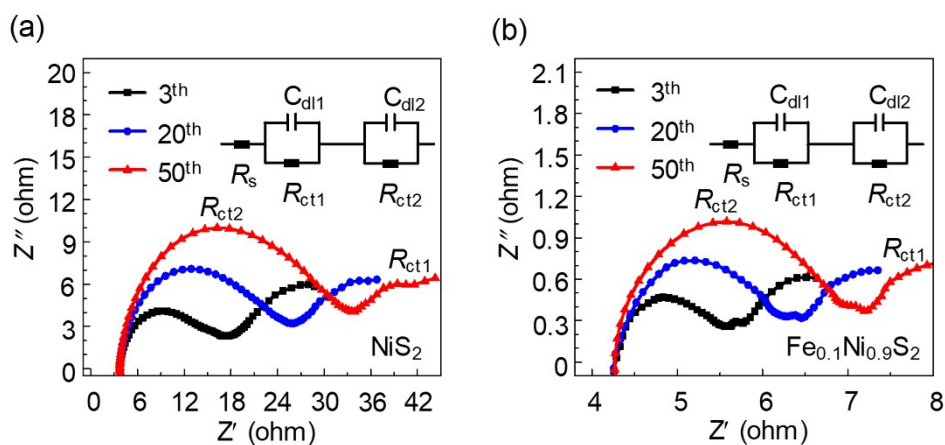


Fig. S7 Nyquist plots of the EIS at potential of +1.63 V vs. RHE for (a) NiS₂ after 3, 20 and 50 cycles of OER measurements; (b) Fe_{0.1}Ni_{0.9}S₂ after 3, 20 and 50 cycles of OER measurements; Inset show the equivalent circuit for fitting the data, consisting of an electrolyte resistance (R_s), a charge transfer resistance (R_{ct1}) caused by electron transfer from electrolyte to the catalyst, and a resistance (R_{ct2}) caused by electron transfer from Fe_xNi_{1-x}OOH layer to Fe_xNi_{1-x}S₂ layer.

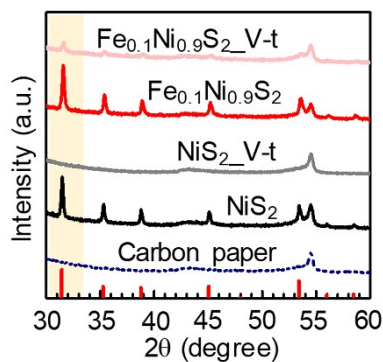


Fig. S8 XRD patterns of the as-synthesized samples (denoted as NiS₂ and Fe_{0.1}Ni_{0.9}S₂) and those of the samples after V-t test (denoted as NiS₂_V-t and Fe_{0.1}Ni_{0.9}S₂_V-t).

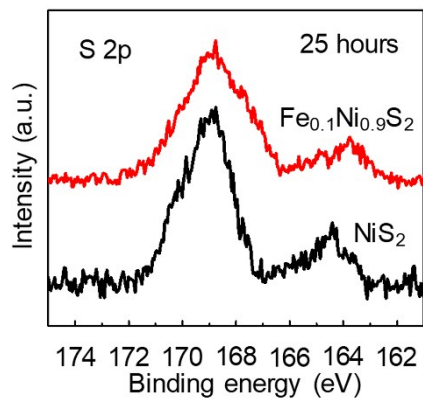


Fig. S9 S 2p XPS spectra for NiS₂ and Fe_{0.1}Ni_{0.9}S₂ after 25 hours stability test.

Table S2 Lattice parameters and the bond length of Fe_xNi_{1-x}S₂ (x=0, 0.05, 0.10 and 0.20) and FeS₂. The shorter Ni/Fe-S bond lengths suggest larger Ni/Fe-S binding energies, and thereby higher energy barrier to break Ni/Fe-S bonds for transformation of Fe_xNi_{1-x}S₂ into Fe_xNi_{1-x}OOH.

x in Fe _x Ni _{1-x} S ₂	<i>a</i> (Å)	Ni-S (Å)	S-S (Å)	Fe-S (Å)
0.00	5.679	2.400	2.038	-
0.05	5.677	2.398	2.046	-
0.10	5.674	2.396	2.048	-
0.20	5.667	2.390	2.077	-
FeS ₂ ¹	5.404	-	2.171	2.259

Reference

1. M. Elliott, *J. Chem. Phys.*, 1960, **33**, 903-905.